


# Laser Intensity Effect on Polyynes Synthesis in Liquid Hydrocarbons

Vitali V. Kononenko <sup>1,\*</sup> , Natalia R. Arutyunyan <sup>1</sup>, Kuralay K. Ashikkalieva <sup>1</sup>, Evgeny V. Zavedeev <sup>1</sup>, Taras V. Kononenko <sup>1</sup>, Ekatherina V. Akhlyustina <sup>2</sup> and Vitaly I. Konov <sup>1</sup>

<sup>1</sup> Prokhorov General Physics Institute of the Russian Academy of Sciences, Vavilov Street 38, 119991 Moscow, Russia; nata@kapella.gpi.ru (N.R.A.); taras.kononenko@nsc.gpi.ru (T.V.K.)

<sup>2</sup> National Research Nuclear University MEPhI, Kashirskoye Shosse 31, 115409 Moscow, Russia

\* Correspondence: vitali.kononenko@nsc.gpi.ru

**Abstract:** Laser synthesis of polyynes molecules  $C_{2n}H_2$  ( $n > 2$ ) in liquid hydrocarbons is a complex process in which intense pulsed radiation decomposes the initial carbon-containing substance (the hydrocarbon solvent itself or the solid carbon particles in a suspension). Notwithstanding the fact that the mechanism of pulsed laser ablation in liquids (PLAL) is widely accepted, the effect of the laser parameters on laser-driven polyynes formation is still not understood in detail. Here, we report a study of the polyynes yield as a function of the laser field intensity and exposure dose. Several carbon-containing liquids, including pure n-hexane, pure ethanol, and graphite powder suspended in ethanol, were treated with tightly focused picosecond IR radiation (wavelength of 1064 nm, pulse duration of 10 ps). The synthesis rate was characterized by UV-vis optical absorption spectroscopy. The yields of the polyynes were found to vary in exact accordance with the value of the absorbed laser energy, following specific nonlinear or linear laws. The influence of the laser intensity on the partial concentration of polyynes in the solution was analyzed.

**Keywords:** laser synthesis of polyynes; laser-induced breakdown; linear carbon chains; pulsed laser ablation in liquids; liquid hydrocarbons



**Citation:** Kononenko, V.V.; Arutyunyan, N.R.; Ashikkalieva, K.K.; Zavedeev, E.V.; Kononenko, T.V.; Akhlyustina, E.V.; Konov, V.I. Laser Intensity Effect on Polyynes Synthesis in Liquid Hydrocarbons. *Photonics* **2023**, *10*, 1100. <https://doi.org/10.3390/photonics10101100>

Received: 21 August 2023

Revised: 22 September 2023

Accepted: 28 September 2023

Published: 29 September 2023



**Copyright:** © 2023 by the authors. Licensee MDPI, Basel, Switzerland. This article is an open access article distributed under the terms and conditions of the Creative Commons Attribution (CC BY) license (<https://creativecommons.org/licenses/by/4.0/>).

## 1. Introduction

Over the decades, laser-induced breakdown (LIB) has remained a phenomenon of great scientific and technological interest. One of the reasons for this is the extraordinary physical conditions that can be realized in the tightly focused laser beam, especially with an ultrafast laser. In both gaseous and condensed media, the temperature, pressure, and ionization levels are so high that chemical bonds are easily broken and new molecules and crystals (including those that have never existed in nature) are formed. In this way, for example, fullerenes were obtained [1]. Carbon-rich substances are of special interest because of the great chemical diversity of carbon compounds.

In particular, in recent years, polyynes have attracted significant attention due to a number of reasons: the perspectives in nanoelectronic devices [2,3], the search for carbyne (the hypothetical linear form of carbon [4]), etc. Polyynes are long-chain carbon molecules  $C_{2n}H_2$  ( $n > 2$ ) in which triple ( $C\equiv C$ ) and single ( $C-C$ ) bonds alternate and are terminated by two hydrogen atoms. Polyynes can be synthesized chemically [5,6] or by arc discharge [7]. However, laser-driven synthesis of polyynes molecules, achieved in both an ablated plume of a solid carbon target [8,9] and in liquid solvents [10], remains a widely accepted and effective technique. Two different approaches to pulsed laser ablation in liquids (PLAL) have been widely used for polyynes production. The first approach uses laser ablation of carbonaceous solid particles, i.e., graphite powder, fullerenes, etc. [10–12]. More recently, ultrafast lasers have been used to directly ablate a hydrocarbon liquid, thereby stimulating the formation of linear carbon chains (LCCs) [13,14]. Note that in addition to liquid hydrocarbons, water is used as a solvent for polyynes, thus reducing the toxicity of the final product [15,16].

Despite the abundance of data on both approaches and the many reviews devoted to laser synthesis of LCCs [6,17–19], the mechanism of laser-driven polyynes formation is still not understood in detail. The intuitive model implies that LIB stimulates the disruption of matter, producing a number of radicals and ions:  $H^+$ ,  $C^+$ ,  $CH^+$ ,  $C_2^+$ ,  $C_2H^+$ , etc. Relaxation after laser excitation makes these dissociation products react with each other. Some of the newly formed molecules appear linear. There are also secondary reactions where C atoms are incorporated into existing chains, making them longer [10,20].

This plausible mechanism has not yet been verified as consistent with the physics of laser-induced ionization of liquids. Meanwhile, some experimental results seem to be contradictory in the LIB context. For example, a strong dependence of the polyyne generation efficiency on the radiation wavelength has been reported. Matsutani et al. found that the PLAL of fullerenes by IR radiation resulted in much faster LCC generation compared to UV radiation [21], while under similar conditions, polyynes were produced only by UV radiation [11]. Surprisingly, Tsuji et al. showed that LCC generation occurs in the absence of visible plasma inside a liquid. Moreover, the generation process under UV irradiation does not depend on the laser fluence and can occur without focusing [10], suggesting the purely photochemical nature of LCC formation.

Similar discrepancies and puzzles can be resolved by studying the relationship between the laser breakdown process in a particular solvent or suspension and the rate of polyyne formation under these conditions in detail. Here, we study the dependence of the polyyne yield on the exposure dose and the intensity of the focused laser beam. The corresponding experimental data are rather scarce [22]. Several carbon-containing liquid media, including pure n-hexane, pure ethanol, and an ethanol suspension of graphite particles, were exposed to prolonged picosecond (ps) IR irradiation. The picosecond pulse duration was a compromise between long (nanosecond) and ultrashort (femtosecond) durations. On the one hand, the picosecond pulses are short enough to still provide high nonlinear absorption in the transparent hydrocarbons and cause stable LIB that does not require the development of an electron avalanche. On the other hand, in the carbonaceous suspensions, the radiation undergoes a remarkable attenuation before it reaches the laser waist. Furthermore, a picosecond pulse of comparable energy was expected not to initiate LIB in the hydrocarbon medium itself, but to ablate only the graphite particles, thus enhancing their dominant role in the polyyne production process.

## 2. Materials and Methods

Ablation of liquid hydrocarbons was performed using a fiber-based diode-pumped solid-state laser (Huaray, Wuhan, China) emitting picosecond ( $\tau = 10$  ps) IR ( $\lambda = 1064$  nm) pulses at a repetition rate of 500 kHz. The beam was focused with a single aspherical lens (NA = 0.3) in the center of a 5 mL fused silica cell. The Gaussian beam radius in the focal plane was  $\approx 2$   $\mu\text{m}$  at the  $1/e$  level. The Rayleigh length of the beam focused in the liquid was estimated to be 20  $\mu\text{m}$ . The average nominal power of the laser was 50 W and the pulse energy reached  $\sim 100$   $\mu\text{J}$ . The laser intensity was varied; the pulse energy was reduced and controlled with a half-wave plate and a Glan polarizer. Irradiation was performed without beam scanning over the target, and the ultra-high repetition rate led to a specific regime of cavitation of the liquid, which completely blocked the laser radiation for  $\sim 1$  s after the first laser shot (this phenomenon will be reported elsewhere). To avoid this supercavitation, the laser was operated at a repetition rate of 10 kHz in the reported experiments.

First, pure n-hexane and ethanol (both 99% purity, fluorometry grade) were used for LCC synthesis. Second, graphite suspensions were prepared for the same purpose. Graphite flakes were milled from a piece of pyrolytic graphite. The resulting  $\sim 10$   $\mu\text{m}$  pieces were suspended in ethanol and milled again for 1 h using a 200 W power ultrasonic tool. The solutions were then allowed to settle for 1 h and filtered. The final 0.4 mg/mL suspensions contained graphite granules of approximately  $\sim 1$   $\mu\text{m}$ . Such a concentration corresponds to  $\sim 0.2 \cdot 10^9$  particles per  $\text{cm}^3$ . This means that  $\sim 0.2$  particles occupy the volume of the laser beam waist ( $\sim 200$   $\mu\text{m}^3$ ). This is sufficient to effectively treat the particles

rapidly drifting in the liquid, which itself remains semi-transparent. Optical absorption spectra of the carbonaceous solutions before and after laser irradiation were recorded using a Perkin Elmer Lambda 950 double-beam spectrophotometer in the range of 180 nm to 1100 nm. Spectra were measured 10 min immediately after laser treatment.

### 3. Results and Discussion

#### 3.1. Polyynene Synthesis in Pure Hydrocarbons

Figure 1 combines the data describing the kinetics and yield of polyynene synthesis in pure n-hexane. Typical absorption spectra obtained after  $10^6$  pulse irradiation are shown in Figure 1a. They show two prominent peaks—215 nm and 225 nm—corresponding to the vibrational structure of the  $C_8H_2$  polyynene [10,23]. Longer chains are rather absent; very weak traces of the absorption bands can be found in the 240–320 nm region.

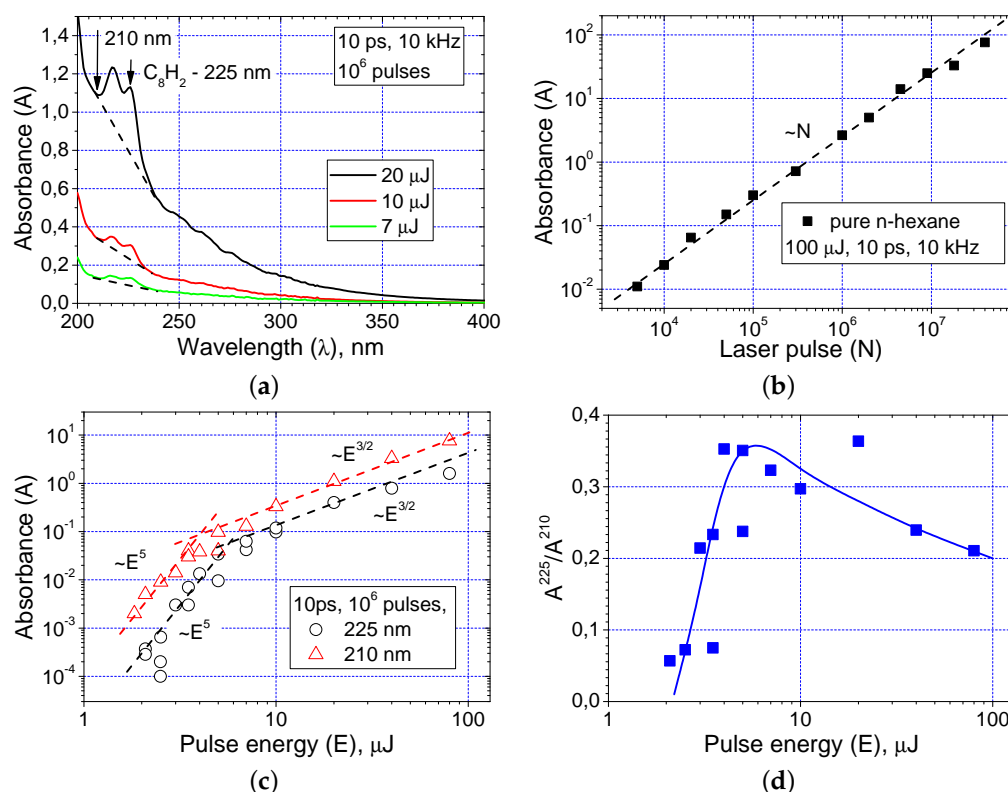


**Figure 1.** LCC formation in n-hexane: (a) Optical absorption spectra after laser treatment with different pulse energies. The first  $C_8H_2$  absorption peak (225 nm) and the 210 nm wavelength used for further characterization of the by-product amount are marked. The black dashed lines indicate the background used to calculate the magnitude of the specific polyynene peak. (b) Dependence of the magnitude of the 225 nm peak ( $A^{225}$ ) on the number of pulses. The pulse energy is 100  $\mu J$ . (c) Absorbances at 225 nm ( $A^{225}$ ) and 210 nm ( $A^{210}$ ) as a function of pulse energy. The irradiation dose is  $10^6$  pulses. The dashed lines show the power law dependencies with exponent factors of 5 and 3/2. (d) Pulse energy dependence of the  $A^{225} / A^{210}$  ratio.

To characterize the kinetics of LCC formation, the effects of laser intensity and dose on the magnitude of the absorbance peak at 225 nm ( $A^{225}$ ) were deduced from the spectra (the black dashed lines in Figure 1a show the deduced background). The absorbance of the solution outside the LCC peaks at 210 nm ( $A^{210}$ ) was used to characterize the residual by-products formed with the polyynes during laser treatment. Below, the ratio of the specified absorbances ( $A^{225} / A^{210}$ ) is analyzed to investigate the intensity effect on the partial concentration of the produced polyynes, i.e., the fraction of polyynes in the mixture of straight-chain alkanes, polycyclic aromatic hydrocarbons, carbon nanostructures, etc., produced in the laser field. The dependence of the 225 nm peak magnitude on the irradiation

tion dose was quite linear, at least up to  $4 \cdot 10^7$  pulses (Figure 1b). No saturation, as might be expected in re-irradiation of previously produced chains, was found.

The dependence of 225 nm and 210 nm absorbances on the laser pulse energy is shown in Figure 1c. The character of the curves is identical within the energy range used, supporting the idea that the LCCs are one of the carbon derivatives formed from laser-disrupted molecules of the hydrocarbon. In particular, both yields have two distinct branches located in the low ( $E < 5 \mu\text{J}$ ) and high ( $E > 5 \mu\text{J}$ ) energy ranges. At low energies, the yields of polyynes and by-products follow a power law with an exponent of 5. At high energies, the exponent coefficient drops to 3/2. Again, no saturation was found. The curves are quite monotonous; the higher the laser intensity, the more molecules are destroyed and the more polyynes and by-products are produced.

The strong nonlinearity is obviously due to the nonlinear absorption of pure hexane, which is transparent in the NIR region of the spectrum and requires at least five photons to reliably absorb laser radiation in the Urbach tail (the absorption edge in n-hexane is about 220 nm). The weak nonlinearity is less obvious and is attributed to the plasma–radiation interaction. The reason for this is the strong saturation of a number of electron–hole pairs ( $N_{eh}$ ) excited by the laser field. In liquids, this saturation occurs at the level of  $N_{eh} \sim 10^{18}\text{--}10^{19} \text{ cm}^{-3}$  [24]. This effect is referred to as “intensity clamping” [25], which means that plasma defocusing prevents the focusing and self-focusing of the radiation, thus stopping an increase in laser fluence inside the LIB zone above a certain value. Under these conditions, the maximum value of  $N_{eh}$  does not increase with pulse energy, while both the diameter and the length of this zone increase as  $D \sim L \sim \sqrt{E}$  [26]. In other words, starting from  $E \approx 5 \mu\text{J}$ , the concentration of photo-excited bonds does not grow with increasing laser energy, but the volume of excited liquid does and thus the amount of substance involved in the reaction grows as  $D^2 \cdot L \sim E^{3/2}$ .

Compared to the absorbance curves, the  $A^{225}/A^{210}$  ratio behaves in a more sophisticated way (Figure 1d). It has a clear maximum located at  $\approx 5 \mu\text{J}$ , which coincides with the inflection point of the absorbance curves. At low laser intensities, the partial concentration of polyynes is quite low compared to other products of the PLAL process. When the pulse energy exceeds  $5 \mu\text{J}$ , the relative proportion of LCCs gradually decreases. We tentatively suggest that this dependence is a result of certain features of n-hexane decomposition in the laser field. The decomposition involves cleavage of C–C and C–H bonds. At a low laser intensity, the molecules remain only partially dehydrated and the LCC yield is predictably low. If the dehydration rate is higher than the C–C cleavage rate, then at some higher laser intensity, the C–H bonds appear to be destroyed while the carbon skeleton of the n-hexane molecule remains almost intact. This is an optimal starting condition to obtain the maximum number of  $\text{C}_8\text{H}_2$  chains. Finally, an excessive laser intensity causes excessive C–C cleavage, the appearance of a number of short molecular fragments, and a decrease in the probability of polyynes polymerization. The complete absence of  $\text{C}_{10}\text{H}_2$  and longer molecules favors this mechanism.

### 3.2. Polyynes Synthesis in Graphitic Suspension

The above results suggest that in the case of a hydrocarbon suspension of a carbon-based material, the source of carbon atoms could be related to either a solid carbon phase or the hydrocarbon liquid itself. To simplify the analysis of laser-treated hydrocarbon suspensions of graphite, ethanol was chosen as the solvent, which itself provides the minimum amount of LCCs. Figure 2 shows the absorption spectrum of laser-treated pure ethanol compared to n-hexane. The  $\text{C}_8\text{H}_2$ -related absorption peaks in ethanol were found to be more than 10 times lower than in n-hexane. The absorbance of longer LCCs was within the noise level. Note also that the kinetics of polyynes synthesis in ethanol and the laser intensity effect were quite similar to the n-hexane case.

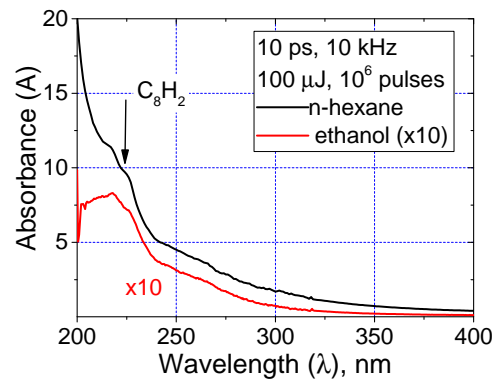


**Figure 2.** Comparison of pure n-hexane and ethanol spectra after  $10^6$  pulse irradiation of  $100 \mu\text{J}$  energy. The ethanol absorbance is  $10\times$  scaled for clarity.

The main data on polyynes formation in the graphite–ethanol suspension are shown in Figure 3. In contrast to the pure hydrocarbons, the typical absorption spectrum of the suspension after laser irradiation contains a number of distinct peaks related to the absorption bands of polyynes up to  $\text{C}_{16}\text{H}_2$  (Figure 3a). As with pure n-hexane, the kinetics of the 225 nm peak were linear (Figure 3b). No saturation caused by depletion of the graphite phase was found.

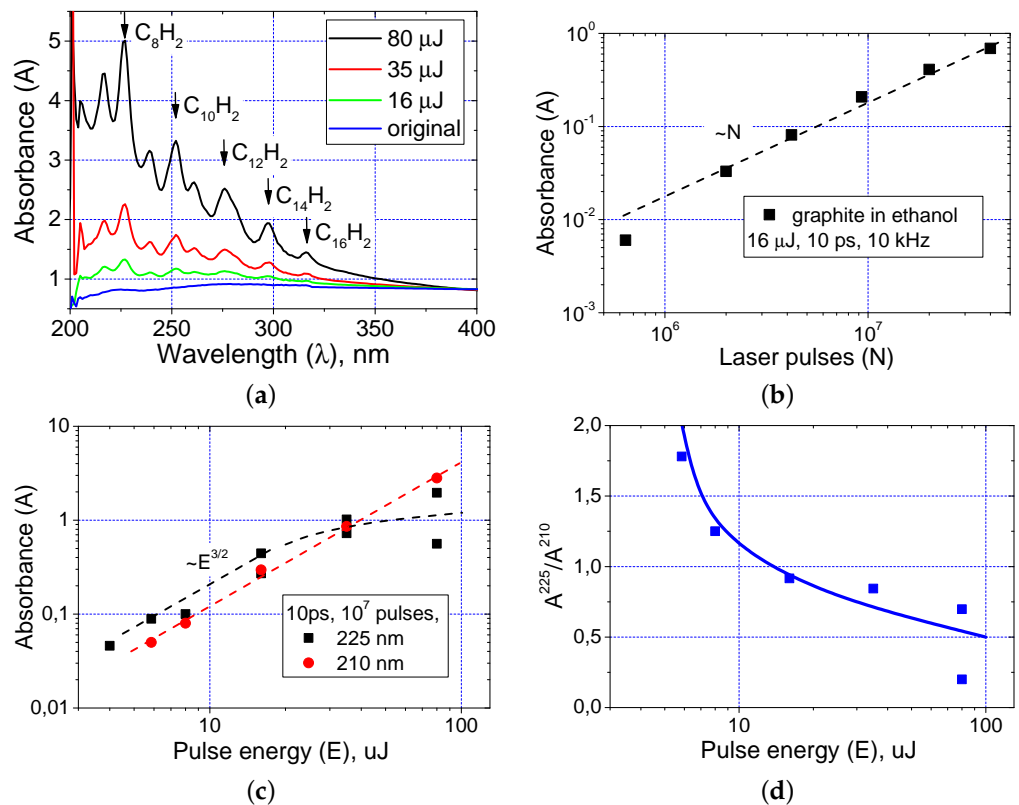


**Figure 3.** LCC formation in the graphite–ethanol suspension: (a) Absorption spectra before and after laser treatment at different laser energies ( $10^7$  pulses). The polyynes peaks ( $\text{C}_8\text{H}_2\text{--C}_{16}\text{H}_2$ ) are marked. (b) Linear dependence of the absorbance at 225 nm ( $A^{225}$ ) on the number of laser pulses. (c) Dependence of the absorbance at 225 nm ( $A^{225}$ ) and 210 nm ( $A^{210}$ ) on the pulse energy. The irradiation dose is  $10^7$  pulses. (d) Pulse energy dependence of the  $A^{225}/A^{210}$  ratio.

The dependencies of the absorbance on the laser pulse energy (Figure 3c) are simpler than for the pure hydrocarbons. Polyyne synthesis started at the threshold energy of  $E \approx 4 \mu\text{J}$ . Until the pulse energy reached  $\approx 30 \mu\text{J}$ , the yields of polyynes and by-products

follow a power law with an exponent of  $3/2$ . The mechanism is obviously the same as in the case of pure solvent—the intensity clamping effect in a liquid. Similarly, at a high excitation level, the laser radiation cannot penetrate the plasma generated in the ethanol and defocuses, leading to an expansion of the LIB volume with increasing pulse energy. At a lower energy ( $E < 4 \mu\text{J}$ ), the one-photon absorption apparently cannot deposit enough energy for graphite ablation and subsequent polyynes formation. It is informative to note that regardless of the linear energy dissipation mechanism, the LCC yield is lower in the case of the graphite suspension. After  $10^6$  pulses of  $20 \mu\text{J}$  energy, the absorbance of n-hexane reaches  $A_{225} \approx 0.3$  compared to  $A_{225} \approx 0.07$  for the graphite suspension. (The latter value is calculated from the data shown in Figure 3b, taking into account the linearity between the number of laser pulses and the laser-induced absorbance).

Note also that from the energy of  $\sim 20 \mu\text{J}$ , there is a clear saturation of the polyynes yield curve, while the by-product yield follows a power law. Furthermore, the  $A^{225}/A^{210}$  ratio indicates that the partial concentration of polyynes decreases over the whole laser energy range, starting from the ablation threshold (Figure 3d). We believe that such a dependence, as in the case of pure n-hexane, is caused by excessive C-C bond cleavage. Presumably, the closer the laser energy is to the PLAL threshold, the longer the carbon chain fragments released during graphite ablation. The intensity effect on the partial concentration of polyynes in the graphite suspension is sufficiently strong; the  $A^{225}/A^{210}$  ratio drops from  $\sim 2.0$  to  $\sim 0.2 \div 0.6$ , a typical value for pure hydrocarbons. Therefore, the strategy of PLAL synthesis in solutions with a high content of long polyynes should be based on relatively low energy ( $\sim 5 \mu\text{J}$ ) lasers with a maximum pulse repetition rate ( $\sim 1 \text{ MHz}$ ).

#### 4. Conclusions

The yield of polyynes synthesized in the liquid hydrocarbons varies in strict accordance with the intensity of the picosecond laser breakdown in solution. For pure hydrocarbons, such as n-hexane or ethanol, two regimes were observed. At low laser intensities, the LCC yield is proportional to the fifth power of the pulse energy, which is defined by the order of the nonlinear absorption in the liquid. At higher laser intensities ( $E > 5 \mu\text{J}$ ), the nonlinearity of the radiation–liquid interaction stimulates the development of an intensity clamping effect, leading to strong saturation of the laser plasma concentration in the LIB zone. The relatively slow ( $\sim E^{3/2}$ ) growth of polyynes production in this regime is caused by the growth of the LIB volume. For suspensions of a linearly absorbing solid carbon phase (graphite), a strong nonlinear branch disappears as expected. Thus, the experiments suggest that the rate of polyynes synthesis is mainly determined by the mechanism of laser energy dissipation in the carbon source phase. This confirms the well-known mechanism of laser-driven LCC formation, which involves two stages: (i) laser ionization and production of radicals, molecular fragments, ions, etc., and (ii) subsequent relaxation involving various chemical reactions, in particular polymerization of polyynes.

More subtle findings were derived from the analysis of LCC and by-product amounts and can be summarized as follows. As the laser intensity increases, the LCC yield in the pure hydrocarbons first increases relative to the by-product yield and then decreases. The optimum laser energy was found to be  $E \approx 5 \mu\text{J}$ . This increase is attributed to the necessary dehydrogenation of alkane molecules. The most likely reason for the decrease is excessive laser-induced decomposition of the parent molecules. On the other hand, in graphite suspensions, the ratio of polyynes to by-product changes monotonically with laser intensity; the higher the laser energy, the lower the relative amount of LCCs in the treated suspension. This is probably the result of the same effect—excessive laser-induced decomposition of the graphite lattice. In other words, the lowest laser intensity, just above the threshold, produces the longest polyynes with the least amount of by-products. However, the synthesis rate is quite modest in this case.

**Author Contributions:** Conceptualization, V.V.K.; investigation, N.R.A. and E.V.Z.; resources K.K.A. and E.V.A.; data curation, T.V.K.; writing—original draft preparation, V.V.K.; supervision, V.I.K. All authors have read and agreed to the published version of the manuscript.

**Funding:** This research was funded by the Russian Science Foundation, grant no. 19-12-00255-P.

**Institutional Review Board Statement:** Not applicable.

**Informed Consent Statement:** Not applicable.

**Data Availability Statement:** Data available on request.

**Conflicts of Interest:** The authors declare no conflict of interest.

### Symbols and Abbreviations

The following symbols and abbreviations are used in this manuscript:

$N$	laser pulse number
$E$	laser pulse energy
$A$	optical absorbance
$N_{eh}$	number of electron–hole pairs
PLAL	pulsed laser ablation in liquid
LIB	laser-induced breakdown
LCC	linear carbon chain

### References

1. Kroto, H.W.; Heath, J.R.; O'Brien, S.C.; Curl, R.F.; Smalley, R.E. C60: Buckminsterfullerene. *Nature* **1985**, *318*, 162–163. [[CrossRef](#)]
2. Paul, F.; Lapinte, C. Organometallic molecular wires and other nanoscale-sized devices: An approach using the organoiron (dppe) Cp\* Fe building block. *Coord. Chem. Rev.* **1998**, *178*, 431–509. [[CrossRef](#)]
3. Bryce, M.R. A review of functional linear carbon chains (oligoynes, polyyynes, cumulenes) and their applications as molecular wires in molecular electronics and optoelectronics. *J. Mater. Chem. C* **2021**, *9*, 10524–10546. [[CrossRef](#)]
4. Eisler, S.; Slepko, A.D.; Elliott, E.; Luu, T.; McDonald, R.; Hegmann, F.A.; Tykwinski, R.R. Polyyynes as a model for carbyne: Synthesis, physical properties, and nonlinear optical response. *J. Am. Chem. Soc.* **2005**, *127*, 2666–2676. [[CrossRef](#)] [[PubMed](#)]
5. Johnson, T.; Walton, D. Silylation as a protective method in acetylene chemistry: Polyyne chain extensions using the reagents, Et3Si (C-C) mH (m = 1, 2, 4) in mixed oxidative couplings. *Tetrahedron* **1972**, *28*, 5221–5236. [[CrossRef](#)]
6. Januszewski, J.A.; Tykwinski, R.R. Synthesis and properties of long [n] cumulenes (n > 5). *Chem. Soc. Rev.* **2014**, *43*, 3184–3203. [[CrossRef](#)] [[PubMed](#)]
7. Cataldo, F. Synthesis of polyyynes in a submerged electric arc in organic solvents. *Carbon* **2004**, *42*, 129–142. [[CrossRef](#)]
8. Heath, J.; Zhang, Q.; O'Brien, S.; Curl, R.; Kroto, H.; Smalley, R. The formation of long carbon chain molecules during laser vaporization of graphite. *J. Am. Chem. Soc.* **1987**, *109*, 359–363. [[CrossRef](#)]
9. Taguchi, Y.; Endo, H.; Kodama, T.; Achiba, Y.; Shiromaru, H.; Wakabayashi, T.; Wales, B.; Sanderson, J. Polyyne formation by ns and fs laser induced breakdown in hydrocarbon gas flow. *Carbon* **2017**, *115*, 169–174. [[CrossRef](#)]
10. Tsuji, M.; Tsuji, T.; Kuboyama, S.; Yoon, S.H.; Korai, Y.; Tsujimoto, T.; Kubo, K.; Mori, A.; Mochida, I. Formation of hydrogen-capped polyyynes by laser ablation of graphite particles suspended in solution. *Chem. Phys. Lett.* **2002**, *355*, 101–108. [[CrossRef](#)]
11. Tsuji, M.; Kuboyama, S.; Matsuzaki, T.; Tsuji, T. Formation of hydrogen-capped polyyynes by laser ablation of C60 particles suspended in solution. *Carbon* **2003**, *41*, 2141–2148. [[CrossRef](#)]
12. Arutyunyan, N.R.; Fedotov, P.V.; Kononenko, V.V. Laser synthesis and stability of one-dimensional polyyne carbon chains in liquid media. *J. Nanophotonics* **2016**, *10*, 012519. [[CrossRef](#)]
13. Sato, Y.; Kodama, T.; Shiromaru, H.; Sanderson, J.; Fujino, T.; Wada, Y.; Wakabayashi, T.; Achiba, Y. Synthesis of polyyne molecules from hexane by irradiation of intense femtosecond laser pulses. *Carbon* **2010**, *48*, 1673–1676. [[CrossRef](#)]
14. Wesolowski, M.J.; Kuzmin, S.; Moores, B.; Wales, B.; Karimi, R.; Zaidi, A.A.; Leonenko, Z.; Sanderson, J.H.; Duley, W.W. Polyyne synthesis and amorphous carbon nano-particle formation by femtosecond irradiation of benzene. *Carbon* **2011**, *49*, 625–630. [[CrossRef](#)]
15. Shin, S.K.; Song, J.K.; Park, S.M. Preparation of polyyynes by laser ablation of graphite in aqueous media. *Appl. Surf. Sci.* **2011**, *257*, 5156–5158. [[CrossRef](#)]
16. Peggiani, S.; Facibeni, A.; Marabotti, P.; Vidale, A.; Scotti, S.; Casari, C.S. A single liquid chromatography procedure to concentrate, separate and collect size-selected polyyynes produced by pulsed laser ablation in water. *Fullerenes Nanotub. Carbon Nanostructures* **2023**, *31*, 224–230. [[CrossRef](#)]
17. Yogesh, G.K.; Shukla, S.; Sastikumar, D.; Koinkar, P. Progress in pulsed laser ablation in liquid (PLAL) technique for the synthesis of carbon nanomaterials: A review. *Appl. Phys. A* **2021**, *127*, 810. [[CrossRef](#)]

18. Marabotti, P.; Peggiani, S.; Vidale, A.; Casari, C.S. Pulsed laser ablation in liquid of sp-carbon chains: Status and recent advances. *Chin. Phys. B* **2022**. [[CrossRef](#)]
19. Zhang, K.; Zhang, Y.; Shi, L. A review of linear carbon chains. *Chin. Chem. Lett.* **2020**, *31*, 1746–1756. [[CrossRef](#)]
20. Zaidi, A.; Hu, A.; Henneke, D.; Duley, W. Femtosecond laser irradiation of liquid alkanes: Mechanism of polyynes formation. *Chem. Phys. Lett.* **2019**, *723*, 151–154. [[CrossRef](#)]
21. Matsutani, R.; Inoue, K.; Wada, N.; Kojima, K. Wavelength dependence of polyynes preparation by liquid-phase laser ablation using pellet targets. *Chem. Commun.* **2011**, *47*, 5840–5842. [[CrossRef](#)] [[PubMed](#)]
22. Park, Y.E.; Shin, S.K.; Park, S.M. The physical effects on the formation of polyynes by laser ablation. *Chem. Phys. Lett.* **2013**, *568*, 112–116. [[CrossRef](#)]
23. Eastmond, R.; Johnson, T.; Walton, D. Silylation as a protective method for terminal alkynes in oxidative couplings: A general synthesis of the parent polyynes H (C-C) nH (n = 4–10, 12). *Tetrahedron* **1972**, *28*, 4601–4616. [[CrossRef](#)]
24. Kononenko, V.V.; Gololobov, V.M.; Konov, V.I. Dynamics of optical polarizability of liquid water exposed to intense laser light. *Opt. Lett.* **2020**, *45*, 256–259. [[CrossRef](#)]
25. Liu, W.; Petit, S.; Becker, A.; Aközbek, N.; Bowden, C.; Chin, S. Intensity clamping of a femtosecond laser pulse in condensed matter. *Opt. Commun.* **2002**, *202*, 189–197. [[CrossRef](#)]
26. Meader, V.K.; John, M.G.; Rodrigues, C.J.; Tibbetts, K.M. Roles of Free Electrons and H<sub>2</sub>O<sub>2</sub> in the Optical Breakdown-Induced Photochemical Reduction of Aqueous AuCl<sub>4</sub>. *J. Phys. Chem. A* **2017**, *121*, 6742–6754. [[CrossRef](#)]

**Disclaimer/Publisher's Note:** The statements, opinions and data contained in all publications are solely those of the individual author(s) and contributor(s) and not of MDPI and/or the editor(s). MDPI and/or the editor(s) disclaim responsibility for any injury to people or property resulting from any ideas, methods, instructions or products referred to in the content.